



ELSEVIER

26 June 1997

PHYSICS LETTERS B

Physics Letters B 403 (1997) 191–196

Multifragmentation with Brownian one-body dynamics

A. Guarnera^{a,b}, Ph. Chomaz^a, M. Colonna^{a,c}, J. Randrup^d

^a GANIL, B.P. 5027, F-14021 Caen Cedex, France

^b Laboratorio Nazionale del Sud, Viale Andrea Doria, I-95129 Catania, Italy

^c CEA DAPNIA, CE Saclay, F-91191 Gif-sur-Yvette Cedex, France

^d Nuclear Science Division, Lawrence Berkeley National Laboratory, University of California, Berkeley, CA 94720, USA

Received 6 January 1997; revised manuscript received 23 April 1997

Editor: C. Mahaux

Abstract

A first application is made of Brownian One-Body Dynamics to nuclear multifragmentation. A gold nucleus is compressed to double density and then let free to evolve under the combined influence of the effective one-body field and the residual two-body collision processes, with the effects of the fluctuations included whenever local spinodal instability occurs. The system quickly expands into a hollow and unstable configuration which transforms into several intermediate-mass fragments. The analysis of the resulting fragment pattern suggests that the model provides a physically reasonable description of nuclear multifragmentation processes. © 1997 Published by Elsevier Science B.V.

PACS: 24.60.ky; 21.65.+f

Keywords: Multifragmentation; Boltzmann-Langevin theory; Brownian motion; Kinetic equation; Fluctuations; Instabilities

1. Introduction

The investigation of nuclear fragmentation phenomena in heavy-ion collisions poses significant theoretical challenges, since the evolution of a given system typically involves an entire spectrum of physical environments, occurs far from equilibrium, presents instabilities and dynamical bifurcations, and may even lead to the production of additional particles. At intermediate energies, the nuclear Boltzmann equation [1] forms a very successful framework for understanding a variety of features associated with nuclear collisions [2,3]. It describes the development of the nucleon phase-space density in the self-consistent effective one-body field as it is being subjected to the average effect of the residual two-body scatterings. When augmented by a stochastic term representing the

fluctuating effects of the two-body collisions, the resulting Boltzmann-Langevin model is appropriate for addressing processes involving instabilities and bifurcations [4].

Stochastic one-body models have the advantage over the standard mean-trajectory descriptions that they can propagate the system all the way from the initial nuclei, through dynamical bifurcations, and to the assembly of individual (and generally excited) primary fragments.

However, the Boltzmann-Langevin model is still too computer demanding to offer a convenient tool for addressing realistic scenarios. Fortunately, both qualitative physical insight and quantitative results can be obtained with suitable approximations to the full theory. In the approximate methods developed earlier [5,6], the effect of the fluctuations induced by the

two-body collisions on the most important unstable modes is simulated by means of a simple noise of a suitable amplitude. The procedure is implemented at the time when the system enters the spinodal region and fragmentation is due to the amplification of the introduced fluctuations. The main disadvantage of this simple method is that it does not allow to take into account the time dependence of the fluctuation source and cannot be applied to situations in which dynamical effects (such as a very fast expansion, for instance) play a major role.

A particularly simple and powerful approximate tool is provided by the Brownian One-Body (BOB) dynamics model developed recently [7]. The present paper presents the first application of this dynamical approach to nuclear multifragmentation.

Relative to the standard nuclear Boltzmann treatment, the BOB dynamics introduces noise in the mean field whenever the local conditions correspond to spinodal instability. The noise is adjusted so that it would produce the same growth rate as the full Boltzmann-Langevin theory for the most unstable mode in nuclear matter prepared at that density and temperature. Since this local tuning of the Brownian term can be done analytically, the additional numerical effort is only minor and, consequently, the model presents a powerful means for making dynamical simulations of nuclear collisions.

2. Brownian one-body dynamics

In one-body transport theories the system is described in terms of the phase-space density $f(s, t)$, where we use $s \equiv (\mathbf{r}, \mathbf{p})$ to denote a point in phase space, with the measure $ds = 4 d\mathbf{r}d\mathbf{p}/h^3$. In the framework of the Boltzmann-Langevin theory, the time evolution of $f(s)$ is governed by a stochastic equation of motion,

$$\frac{\partial f}{\partial t} = \{h[f], f\} + \bar{I}[f] + \delta I[f]. \quad (1)$$

The first term on the r.h.s. produces the collisionless propagation of f in the self-consistent one-body field described by the effective Hamiltonian $h(s) = \mathbf{p}^2/2m + U(\mathbf{r})$. The second source of evolution, $\bar{I}[f]$, is the term included in the standard BUU description representing the average effect of the residual

Pauli-suppressed two-body collisions. The third term, $\delta I[f]$, is the Langevin term, which accounts for the fluctuating part of the two-body collisions [4].

The basic idea behind the BOB treatment [7] is to approximate the effect of the stochastic collision term by means of a suitable stochastic one-body potential $\delta U(\mathbf{r}, t)$. The corresponding equation of motion is then obtained by making the following replacement in (1),

$$\delta I[f] \rightarrow \delta \bar{I}[f] = -\delta \mathbf{F}[f] \cdot \frac{\partial f}{\partial \mathbf{p}}, \quad (2)$$

where $\delta \mathbf{F}(\mathbf{r}, t) = \partial \delta U / \partial \mathbf{r}$ is the associated Brownian force (having $\langle \delta \mathbf{F} \rangle = 0$). Since the Langevin term in (1) is ordinarily assumed to be Markovian and local in space, the stochastic force is also assumed to be local in time and space. As shown in Ref. [7] for idealized two-dimensional nuclear matter, it is possible to adjust the strength of the correlation function for the Brownian force in such a manner that the agitation of the most unstable modes is well reproduced. This can be achieved by tuning the variance of the Brownian force $\langle \delta \mathbf{F}(\mathbf{r}, t) \delta \mathbf{F}(\mathbf{r}, t) \rangle = 2\bar{D}_0(\mathbf{r}, t)$,

$$\begin{aligned} 2\bar{D}_0(\mathbf{r}, t) = & \frac{4}{3} \left(\frac{3\pi^2}{2} \right)^{2/3} \hbar^2 \frac{N}{\rho^{1/3}} \\ & \times \left\{ \frac{\rho k^2}{m\omega_k^2} \frac{\partial U_k}{\partial \rho} [1 + F_0(k)] \right. \\ & \left. - \frac{2k^2}{m} \frac{\epsilon_F}{\omega_k^2} [1 + F_0(k)]^2 - 1 \right\}. \quad (3) \end{aligned}$$

Here F_0 is the Landau parameter associated with uniform nuclear matter prepared at a density and temperature equal to the local values ρ and T , respectively, and it characterizes the response to harmonic density changes of a given wave number. The most unstable mode has the wave number k and the frequency ω_k . Finally, we have introduced the local collision rate per particle, $N(\rho, T)$.

Thus the BOB method appears to be well suited for studies of multifragmentation by the occurrence of instabilities.

3. Results and discussion

We report here on a first application of the BOB treatment to a three-dimensional nuclear multifrag-

mentation scenario. In order to make contact with earlier studies [8], we consider the disassembly of a gold nucleus that was prepared in a suitably compressed configuration.

If the gold nucleus is initially compressed to twice the normal density, it will expand into a quasi-stationary hollow configuration which is unstable against multifragmentation [8]. A qualitatively similar result was obtained for central collisions of niobium nuclei [9]. For significantly smaller compressions the system will exhibit weakly damped large-amplitude monopole oscillations and eventually settle into a hot compound nucleus. On the other hand, for significantly larger compressions the outwards motion resulting from the release of the compressional energy is sufficient to overcome the cohesive forces of nuclear matter and the system will be torn apart into rapidly receding very light fragments. For our present purposes, it is therefore most instructive to consider the near-critical compression of two. Moreover the formation of such compressed composite sources is observed in several dynamical simulations of actual collisions between heavy ions at intermediate energies [9–11].

The BUU calculations performed in Ref. [8] exhibit a sensitivity to the adopted number of test particles per nucleon, \mathcal{N} . This quantity is a numerical parameter governing the density of the phase-space coverage. In particular, it was found that with $\mathcal{N} = 300$ the spherical symmetry is so well preserved (as it should be mathematically) that the hollow configuration eventually recontracts and no multifragmentation occurs, whereas with $\mathcal{N} = 100$ the coverage is sufficiently coarse to allow the unstable density irregularities to grow, leading to a multifragmented final configuration. In the BOB simulations this sensitivity to numerical parameters is absent because the strength of the stochastic force is larger than the numerical noise.

The evolution of the radial density profile is shown in Fig. 1. It is obtained by performing an angular average for each system and subsequently averaging over a sample of 100 similarly prepared systems. It is clearly seen how the initially uniform density develops a hollow interior, with the matter concentrated within a relatively thin shell that remains nearly stationary for a considerable length of time.

During this stage the matter in the shell condenses into a number of prefragments. As it is shown in Fig. 1,

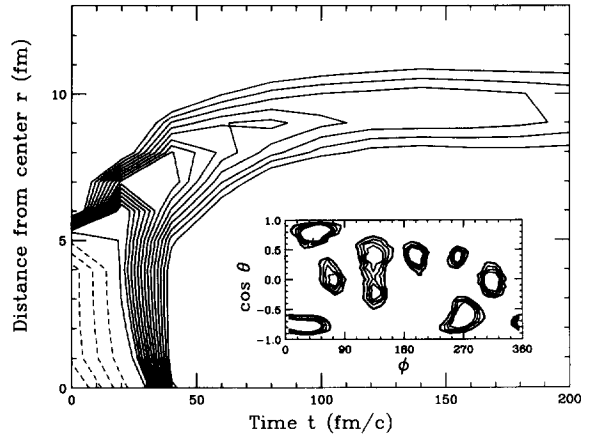


Fig. 1. Evolution of the density profile. The time evolution of the radial density profile is shown in the form of a contour plot. The heavy contour corresponds to normal nuclear density. The density contours are separated by $\Delta\rho = 0.005 \text{ fm}^{-3}$ and dashed contours are employed in the regions of compression. Contour plots of the density $\rho'(\theta, \phi) = 4\pi/A_0 \int r^2 dr \rho(\mathbf{r})$, obtained for a single event at the final time $t = 200 \text{ fm}/c$, are shown in the insert.

at the time $t = 200 \text{ fm}/c$ the prefragments are located in a thin shell of radius $R = 10 \text{ fm}$. As an example of their spatial distribution, we show in the insert of Fig. 1 contour plots of the density $\rho'(\theta, \phi) = \frac{4\pi}{A_0} \int r^2 dr \rho(\mathbf{r})$ calculated for a single event. A_0 indicates the total number of nucleons, $A_0 = 197$. Since the matter distribution is essentially concentrated near a spherical surface, it is natural to analyze the density irregularities in terms of spherical harmonics. This can be conveniently done by introducing multipole moments [8],

$$\alpha_{LM}^{(n)} \equiv \sqrt{4\pi} \int \frac{d\mathbf{r}}{A_0} \rho^{(n)}(\mathbf{r}) Y_{LM}(\hat{\mathbf{r}}). \quad (4)$$

The superscript identifies the particular event n . Since the systems have been sampled from an ensemble that has rotational invariance, all the magnetic components of a given multipolarity are equivalent. It therefore suffices to study the average total strength of a given multipolarity L ,

$$\sigma_L \equiv \left\langle \sum_M |\alpha_{LM}^{(n)}|^2 \right\rangle, \quad (5)$$

where $\langle \cdot \rangle$ denotes the ensemble average. This quantity is a useful measure of the total multipolarity distribution of the fluctuation strength. Its normalization is such that the monopole term is unity, $\sigma_0 = 1$. Furthermore, the higher multipole strength can be obtained

Table 1

Multipole strength of idealized configurations. The multipole coefficients σ_L associated with a number of especially simple multifragment configurations consisting of N touching spheres of equal size. For $N = 4$ the centers form an equilateral tetrahedron (obtained, for example, by occupying every second corner of a cube), for $N = 6$ they are located on the faces of a cube, for $N = 8$ they form the corners of a cube, and for $N = 12a$ they sit on the edges of a cube; for the alternative configuration $N = 12b$, the spheres are centered on the faces of the twelve regular pentagons that form a dodecahedron. These special geometries have also been considered in Ref. [12] where the potential barrier was calculated for each multifragment channel as a function of the root-mean-square size of the configuration

L	$N = 4$	$N = 6$	$N = 8$	$N = 12a$	$N = 12b$
2	0.00	0.00	0.00	0.00	0.00
3	0.10	0	0	0	0
4	0.010	0.060	0.064	0.014	0.00
5	0.00	0	0	0	0
6	0.00	0.00	0.016	0.032	0.030
7	0.00	0	0	0	0
8	0.00	0.00	0.00	0.00	0.00

by performing a Legendre expansion of the two-point reduced angular correlation function,

$$\tilde{\sigma}_{12} = \sum_{L>0} \sigma_L P_L(\cos \theta_{12}), \quad (6)$$

where

$$\tilde{\sigma}_{12} \equiv \int \frac{r_1^2 dr_1}{A_0} \int \frac{r_2^2 dr_2}{A_0} \langle \delta\rho^{(n)}(\mathbf{r}_1) \delta\rho^{(n)}(\mathbf{r}_2) \rangle \quad (7)$$

In order to provide a feeling for the relationship between the multipolarity strength distribution and the underlying multifragment configurations, we show in Table 1 the values of σ_L for a number of especially simple configurations consisting of symmetric arrangements of N touching fragments of equal size. The dominant multipolarity can be roughly predicted by counting the number of fragments along a major circle around the configuration. For example, for $N = 6$ one encounters four fragments as one circles the configuration in the xy plane, and the count is approximately six for the configurations with $N = 12$.

With this preparation, we now turn to the analysis of the sample of 100 multifragmentation events. Fig. 2 shows the multipolarity strength distribution at successive times during the evolution. At the outset, each

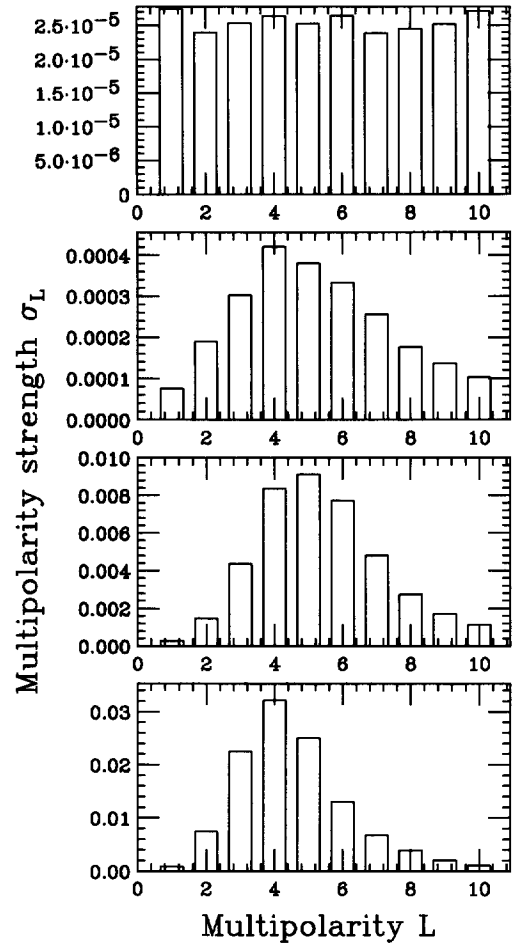


Fig. 2. Multipole strength distribution. The multipole strength coefficients σ_L are shown at various points in time, $t = 0, 60, 120, 180$ fm/c, as the initially compressed gold nucleus expands towards a fragmenting hollow shell. The results are obtained by averaging over 100 events.

mode is agitated to a degree depending on the number of test particles employed. By using $\mathcal{N} = 200$ we ensure that this numerical noise is unimportant relative to the physical noise generated by the two-body collisions. Since the test particles are randomly distributed, the numerical noise is white, yielding a constant (but insignificant) contribution for each multipolarity. The physical noise is also approximately white, as can be seen from the multipole expansion obtained in Ref. [13]. Consequently the different multiplicities are about equally agitated at early times. During the early expansion stage, the bulk of the nucleus is

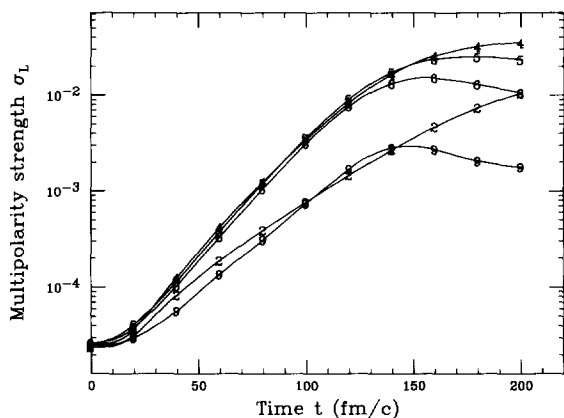


Fig. 3. Time evolution of the multipole coefficients. The time dependence of several multipole strength coefficients σ_L , corresponding to the scenario considered in Fig. 1.

still above the critical density for spinodal decomposition. However, the expanding surface region is unstable, as the dilute matter seeks to increase its binding. This leads to an amplification of the surface irregularities, and determines the initial growth of the multipolarity strengths observed in fig. 2. As the bulk density of the system subsequently enters into the region of spinodal instability, the unstable bulk modes are amplified as well. It should be noticed that, because of the nuclear surface, the monopole mode ($L = 0$) is agitated since the beginning of the process, while the multipolarities are excited by the stochastic force only when the local spinodal instability occurs. Once the system becomes dilute, this favours the rapid growth of the monopole mode and the prompt development of a hollow configuration. Meanwhile, the various multipoles are agitated by the Brownian force and the associated strength starts to grow, with the most unstable modes increasing most rapidly. Once the hollow configuration has been formed, there is little change in the strength distribution, except for a continued overall growth, as the amplified irregularities relatively rapidly condense into a number of intermediate-mass fragments. The multiplicity and the characteristics of the fragments obtained are determined primarily by the dominant multipolarities.

A different view of the time evolution is shown in Fig. 3 in which some of the multipole coefficients presented in Fig. 2 are plotted as functions of time. The early exponential growth characteristic of unstable modes is apparent, and the eventual leveling off at the time when the fragments are fully formed is

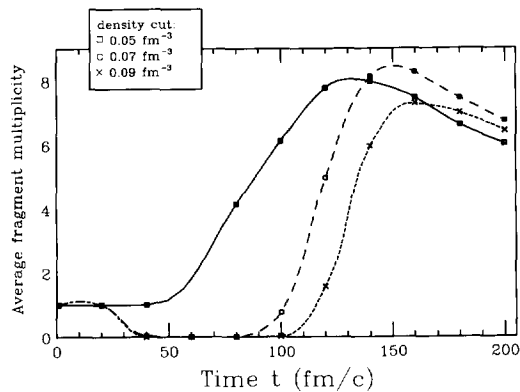


Fig. 4. Fragment multiplicity. The time evolution of the average prefragment multiplicity, as obtained by analyzing that part of the density distribution that exceeds a specified cut-off value, $\rho_{\text{cut}} = 0.05$ (solid), 0.07 (dash), 0.09 (dots) fm^{-3} .

consistent with the magnitudes shown in Table 1. The final multipole strength is concentrated around $L \approx 4$, suggesting a final fragment multiplicity of around $N \approx 6$, based on the insight provided by the idealized configurations shown in Table 1.

This expectation is indeed borne out by a quantitative analysis of the matter density distribution, as illustrated in Fig. 4. By employing a certain density cut-off, it is possible to determine how many distinct pre-fragments are present at each time during a given evolution. Fig. 4 shows the resulting fragment multiplicity as a function of time, as obtained with different cut-off values. At early times it is most instructive to use a fairly large value of the density cut-off, since the system is still well connected (and the “fragments” are then merely local density enhancements). At late times, when the fragments are well separated, and the nucleon vapor has dispersed sufficiently, the fragment analysis is insensitive to the cut-off value. Indeed, we observe a convergence of the results obtained with three different cut-off values at $t \approx 150$ fm/c when the condensation is completed. Moreover, the fragment multiplicity is then indeed around $N \approx 6$, as already surmised from the multipole strength distribution.

We finally show the distribution of fragment sizes. Fig. 5 shows the fragment charge distribution, as obtained at $t = 200$ fm/c with the lowest density cut-off value of $\rho_{\text{cut}} = 0.05 \text{ fm}^{-3}$. We observe a rather broad distribution of fragment sizes, with a concentration near carbon-like fragments. It should be pointed out that a significant fraction of the initial matter is

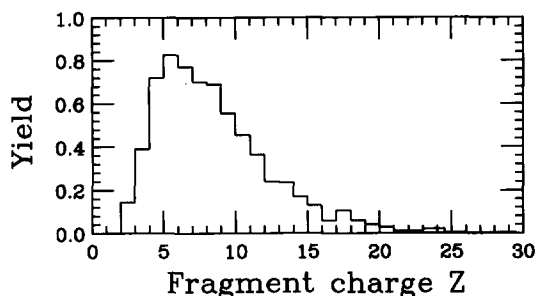


Fig. 5. Fragment charge distribution. The fragment charge distribution as obtained by analyzing the density at time $t = 200$ fm/c with the smallest density cut, $\rho_{\text{cut}} = 0.05 \text{ fm}^{-3}$.

emitted in the form of individual nucleons, or other very light particles, so the matter contained in the intermediate-mass fragments is typically less than half of the total. The emergence of several intermediate-mass fragments is a reflection of the fact that certain unstable multipoles dominate the dynamics. Also, as is evident from the multipolarity strength distribution, the dynamics effectively suppresses the development of high multiplicities, thereby preventing the formation of very small primary fragments.

While the characteristics (such as the wavelength and the growth time) of the most important modes are not very much dependent on the values of density and temperature inside the spinodal region, it should be noticed that the resulting fragment size decreases when diluting the system. Therefore our results depend on the value of the initial compression (and the induced expansion velocity) given to the system. Larger fragments can be obtained for less expanding system, as in the case considered in Ref. [6].

4. Concluding remarks

In this paper, we have presented a first application of the Brownian One-Body dynamics model to nuclear multifragmentation. This model is a recently developed stochastic mean-field description which provides a simple approximation to the Boltzmann-Langevin theory, itself a parameter-free extension of the nuclear Boltzmann equation that incorporates the fluctuating part of the collision integral. Moreover, the Brownian One-Body dynamics can be easily incorporated into existing test-particle implementations of the standard nuclear Boltzmann model and is therefore a very convenient tool for addressing processes in which dynam-

ical bifurcations occur (such processes are beyond the standard treatment which treats only the average evolution).

In order to assess the practical utility of the treatment, we have considered an idealized multifragmentation scenario in which gold nuclei are initially compressed to double density and followed as they expand into hollow configurations that quickly condense into several intermediate-mass fragments, while shedding off a large number of unbound nucleons. The results appear physically reasonable, suggesting that application to actual nuclear collisions is meaningful. Consequently, studies of cases under experimental investigation are planned.

Acknowledgements

This work was supported by the Director, Office of Energy Research, Office of High Energy and Nuclear Physics, Nuclear Physics Division of the US Department of Energy, under Contract No. DE-AC03-76SF00098.

References

- [1] G.F. Bertsch and S. Das Gupta, Phys. Rep. 160 (1988) 190.
- [2] P. Schuck, R.W. Hasse, J. Jaenicke, C. Gregoire, B. Remaud, F. Sebille and E. Suraud, Prog. Part. Nucl. Phys. 22 (1989) 181.
- [3] W. Cassing, V. Metag, U. Mosel and K. Niita, Phys. Rep. 188 (1990) 363.
- [4] S. Ayik and C. Gregoire, Phys. Lett. B 212 (1988) 269; Nucl. Phys. A 513 (1990) 187; J. Randrup and B. Remaud, Nucl. Phys. A 514 (1990) 339.
- [5] M. Colonna, G.F. Burgio, Ph. Chomaz, M. Di Toro and J. Randrup, Phys. Rev. C 47 (1993) 1395.
- [6] A. Guarnera, M. Colonna and Ph. Chomaz, Phys. Lett. B 373 (1996) 267.
- [7] Ph. Chomaz, M. Colonna, A. Guarnera and J. Randrup, Phys. Rev. Lett. 73 (1994) 3512.
- [8] G. Batko and J. Randrup, Nucl. Phys. A 563 (1993) 97.
- [9] W. Bauer, G.F. Bertsch and H. Schulz, Phys. Rev. Lett. 69 (1992) 1888.
- [10] B. Borderie, B. Remaud, M.F. Rivet and F. Sebille, Phys. Lett. B 302 (1993) 15.
- [11] L.G. Moretto, Kin Tso, N. Colonna and G.J. Wozniak, Phys. Rev. Lett. 69 (1992) 1884.
- [12] E. de Lima-Medeiros and J. Randrup, Phys. Rev. C 45 (1992) 372.
- [13] J. Randrup and S. Ayik, Nucl. Phys. A 572 (1994) 489.